Toxicology and Applied Pharmacology **176,** 81–91 (2001)
doi:10.1006/taap.2001.9269, available online at http://www.idealibrary.com on IDEAL®

A Physiologically Based Pharmacokinetic Model for Inhalation and Intravenous Administration of Naphthalene in Rats and Mice

B. A. T. Willems, R. L. Melnick, M. C. Kohn, and C. J. Portier

Laboratory of Computational Biology and Risk Analysis, National Institute of Environmental Health Sciences, Research Triangle Park, North Carolina 27709

Received April 13, 2001; accepted July 27, 2001

A Physiologically Based Pharmacokinetic Model for Inhalation and Intravenous Administration of Naphthalene in Rats and Mice. Willems, B. A. T., Melnick, R. L., Kohn, M. C., and Portier, C. J. (2001). *Toxicol. Appl. Pharmacol.* **176, 81–91.**

A diffusion limited physiologically based pharmacokinetic model for rats and mice was developed to characterize the absorption, distribution, metabolism, and elimination of naphthalene after inhalation exposure. This model includes compartments for arterial and venous blood, lung, liver, kidney, fat, and other organs. Primary sites for naphthalene metabolism to naphthalene oxide are the lung and the liver. The data used to create this model were generated from National Toxicology Program inhalation and iv studies on naphthalene and consisted of blood time-course data of the parent compound in both rats and mice. To examine the basis for possible interspecies differences in response to naphthalene, the model was extended to describe the distribution and metabolism of naphthalene oxide and the depletion and resynthesis of glutathione. After testing several alternative models, the one presented in this paper shows the best fit to the data with the fewest assumptions possible. The model indicates that tissue dosimetry of the parent compound alone does not explain why this chemical was carcinogenic to the female mouse lung but not to the rat lung. The species difference may be due to a combination of higher levels of naphthalene oxide in the mouse lung and a greater susceptibility of the mouse lung to epoxide-induced carcinogenesis. However, conclusions regarding which metabolite(s) may be responsible for the lung toxicity could not be reached.

Key Words: **PBPK; mathematical modeling; naphthalene; carcinogenicity; glutathione.**

Naphthalene, a volatile aromatic hydrocarbon, is widely used in mothballs and toilet bowl deodorants, in the production of dyes and lubricants (Sittig, 1980), and in veterinary medicine to control lice on livestock and poultry (ATSDR, 1990; Schmeltz *et al.,* 1976). Naphthalene is a natural constituent of coal tar and crude oil and has been identified in cigarette smoke and emissions from fossil fuel combustion. Former coal and oil gasification plants generated large amounts of tar and sludge, which contained substantial amounts of naphthalene and related hydrocarbons. Occupational exposures, including in the aluminum smelting industry, have been reported at about 1100 $\mu g/m^3$ (210 ppb) (Bjorseth *et al.,* 1978). Potential chronic human exposure can occur through contaminated ground water, direct exposure from wastes sites, mobile source emissions, use of mothballs in the house, and cigarette smoking. Naphthalene has been found to cause cataracts and hemolytic anemia in humans (ATSDR, 1990).

The National Institute of Occupational Safety and Health, the Occupational Safety and Health Administration, and the United States Environmental Protection Agency nominated naphthalene for carcinogenicity testing by the National Toxicology Program (NTP) because of the potential chronic human exposure and the lack of adequate carcinogenicity studies in the literature to reach a regulatory decision. A positive carcinogenic response (increased incidences of lung neoplasm in exposed female mice) was found in the NTP mouse inhalation study (NTP, 1992). However, lack of studies with naphthalene in rats via the inhalation route (the major route for human exposure) led the NTP to conduct a carcinogenicity inhalation study in this species (NTP, 2000).

Naphthalene toxicity is highly species, tissue, and cell selective (Mahvi *et al.,* 1977; Plopper *et al.,* 1992; Tong *et al.,* 1981). An oral dose of 50 mg/kg naphthalene induced Clara cell toxicity in mice. Doses that are 8 or 32 times higher do not affect the terminal airways in hamsters or rats, respectively (Plopper *et al.,* 1992). Differences are also observed in the cytotoxicity of naphthalene in the epithelium of the nasal cavity, where the mice and hamsters showed necrosis at higher concentrations (400 mg/kg ip) than rats (200 mg/kg ip) (Plopper *et al.,* 1992). The olfactory region was affected in mice, rats, and hamsters.

The metabolic pathway for naphthalene in mammals has been determined. The first step is the formation of two naphthalene 1,2-oxide enantiomers (1*R*, 2*S*-naphthalene 1,2-oxide and 1*S*, 2*R*-naphthalene 1,2-oxide) by the cytochrome P450 monooxygenase system. Those intermediates may undergo further metabolism to dihydrodiols by epoxide hydrolase enzymes, nonenzymatic rearrangement to 1-naphthol, covalent binding to macromolecules, or formation of glutathione (GSH) conjugates by glutathione *S*-transferase (Kanekal *et al.,* 1991).

0041-008X/01

Physiologically based pharmacokinetic (PBPK) models can provide insight into an organism's physiological mechanisms of response to a chemical (D'Souza and Boxenbaum, 1988). They can be helpful in describing the absorption, distribution, excretion, and biotransformation of the chemical and its metabolites (Hoang, 1995) and can form a basis for extrapolation of toxicological effects from high doses to low doses and across species. A large amount of animal- and chemical-specific data is required for development of PBPK models, which consist of simplified mathematical equations that account for the complex physiological and biochemical processes that affect the behavior of the chemical in a particular species.

Based on both rat and mouse blood time-course data from the NTP inhalation studies on naphthalene, a PBPK model was developed to investigate the absorption, distribution, metabolism, and elimination of naphthalene in these two species. No data are available on GSH levels in animals exposed to naphthalene or tissue partition coefficients for naphthalene and its metabolites. Therefore, the current model is partly based on previously published work. Former PBPK models for naphthalene and naphthalene oxide were developed using *in vitro* data solely; these models did not investigate absorption or metabolic elimination resulting from inhalation exposure (Ghanem and Shuler, 2000; Quick and Shuler, 1999; Sweeney *et al.*, 1996).

MODEL DEVELOPMENT

Available data. Whole blood samples taken from groups of 9 male and 9 female F344/N rats exposed to 10, 30, or 60 ppm naphthalene by inhalation for 5 days per week, 6 h per day were analyzed for naphthalene concentrations at 2 weeks and at 3, 6, 12, and 18 months. Additional groups of 12 male and 12 female rats and $B6C3F_1$ mice were obtained from the same suppliers of animals for the 2-year cancer study (NTP, 2000) (Taconic Laboratory, Germantown, NY). Blood samples from rats were evaluated after a single 6-h inhalation exposure to 10, 30, or 60 ppm plus a 12-min delay for the naphthalene concentration in the chamber to decay to 10% of its target level; blood samples from mice were evaluated after a single 7-h inhalation exposure to 10 or 30 ppm plus the same 12-min delay. Blood was taken at eight time points postexposure for the single-exposure groups (0, 30, 60, 90, 120, 240, 360, and 480 min) and at 6 time points for the multiple exposures (10 ppm: 0, 30, 60, 120, 300, and 480 min; 30 ppm: 0, 30, 90, 300, 480, and 720 min; 60 ppm: 0, 30, 90, 360, 720, and 960 min). Each rat was bled twice. At each time point, blood was taken from up to 3 animals per group, and naphthalene concentrations in whole blood were measured. For the iv study, 12 male and 12 female F344 rats (Taconic Laboratory) were implanted with jugular vein cannulae. After administration of 1, 3, or 10 mg naphthalene/kg doses, blood was collected at 10 time points postexposure for each dose group (1 and 3 mg naphthalene/kg: 2, 5, 10, 20, 40, 60, 120, 240, 360, and 480 min; 10 mg naphthalene/kg: 5, 10, 20, 40, 60, 120, 240, 360, 480, and 720 min). All samples were analyzed by CEDRA Corporation (Austin, TX) using a previously validated high-performance liquid chromatography method with ultraviolet light detection (CEDRA, 1994).

Model structure. A physiologically based pharmacokinetic model representing the uptake, distribution, and metabolism of naphthalene in rats and mice was developed to describe the processes involved in naphthalene toxicokinetics. The model, developed in MATLAB (The Mathworks, 1999), consists of two parts (Fig. 1). The model for naphthalene is diffusion limited (Kohn, 1997) and contains compartments for arterial and venous blood, alveolar space, and tissue and capillary spaces for the lung, liver, kidney, fat, and other organs. Diffusion limitation was added to the model to adequately fit the blood time-course data; a flow-limited model failed to reach the necessary steady-state concentrations of naphthalene in the blood at the end of the exposure period. The compartment for "other" organs represents both slowly and rapidly perfused tissues (e.g., skin, muscle, bone marrow, heart, and brain). Because of the possibility of some minor metabolic action in the kidney, this tissue was not included with the "other" organs. Even though it was later found that there was no need for this separation, as the data could be explained with metabolism in the lung and liver only, the kidney was modeled as a separate tissue. Inhalation of naphthalene from the exposure chamber atmosphere takes place through the alveolar space into the lung. Uptake is modeled as being dependent on the ventilation rate of the animal, permeability of the tissue, and blood flow through the lung. Exchange of naphthalene between the lung capillary blood and the alveolar air is flow limited.

The primary sites for naphthalene metabolism to naphthalene oxide are the lung and liver (Buckpitt *et al.*, 1987). Several methods to match the blood time-course naphthalene data were explored (e.g., Michaelis–Menten kinetics in both lung and liver, noncompetitive inhibition, and competitive inhibition). The best results were obtained by using Michaelis–Menten metabolic pathways in both the lung and liver. An assumption was that the same isoform of the P450 enzyme (presumably P450 2F2 (Buckpitt *et al.*, 1995)) is responsible for the metabolism in the lung and liver. The difference in activity lies in the microsomal protein content of these two tissues. A second assumption was that naphthalene only binds to one site on the P450 enzyme in one conformation. So only two metabolic parameters had to be used in the model, one V_{max} (for both the naphthalene oxide enantiomers, *RS* and *SR*) and one K_m. All the physiological parameters (ventilation rate, cardiac output, tissue volumes, capillary volumes, and blood flow rates to the tissues) used in this model were based on values obtained from the literature (see Table 1 for references) and scaled to the body weights of core study rats (body weight in kilograms).

As tissue partition coefficients were not measured in the experiment, these were predicted from the experimental equilibrium constant for the dissolution of a chemical in solvent ($K_{octanol:water}$) (Hansch *et al.*, 1995) using a linear free energy relationship for chemicals (Abraham *et al.*, 1985; Lyman *et al.*, 1990) and regression equations for the different tissues (Fiserova-Bergerova *et al.*, 1984). The calculated partition coefficients listed in Table 1 are comparable to the ones used by Quick and Shuler (1999) (except for the blood:air coefficient). Maximal metabolic rate constants and permeability constants were estimated by fitting the naphthalene blood time-course data from the inhalation studies. The relative rate of metabolism in the lung vs the liver was quantified by multiplying the fitted V_{max} (per milligram microsomal protein) by the measured microsomal protein content of the respective tissues. Goodness of fit was evaluated using a maximum-likelihood ratio test (Kotz and Johnson, 1983). Equations and an explanation of the abbreviations used are shown in the Appendix and Notations.

The second part of the model (Fig. 1), which includes the distribution and metabolism of naphthalene oxide, is an extension of an existing flow-limited model by Quick and Shuler (1999) with *in vitro* parameter values for epoxide hydrolase and glutathione *S*-transferase activities. Because there were no data available on naphthalene oxide distribution or metabolism from the NTP studies, it is not possible to verify predictions of naphthalene oxide tissue dosimetry based on this model. All metabolic parameters used in the Quick and Shuler model (1999) were kept the same in the model for naphthalene oxide metabolism presented in this paper. In addition, glutathione metabolism, as presented in Quick and Shuler (1999), was replaced by GSH synthesis based on Kohn and Melnick (2000). With this system, GSH production is limited by the activity of γ-glutamyl-cysteine synthetase, which was modeled with Michaelis–Menten kinetics and noncompetitive inhibition by the GSH product (Kohn and Melnick, 2000). All physiological parameters were the same as those used in the current naphthalene model. The kidney and "other tissues" compartment replaced the richly and poorly perfused tissue compartments from Quick and Shuler (1999), respectively. All equations and parameters used

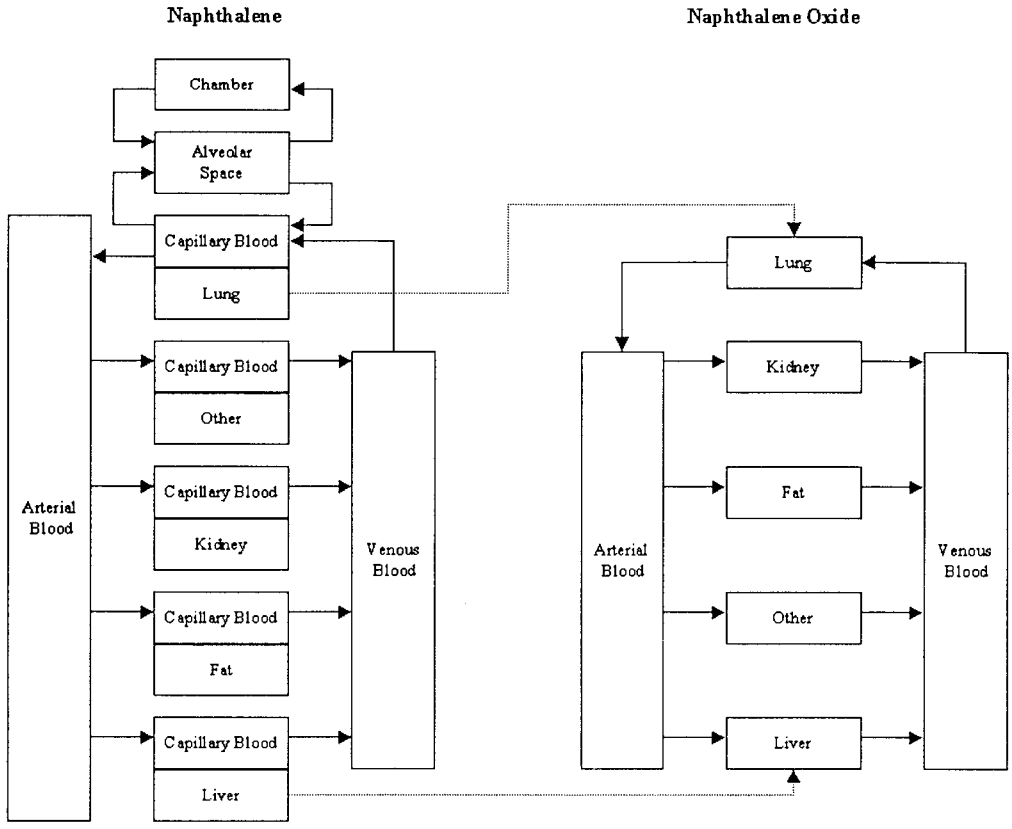

FIG. 1. Pharmacokinetic model for rats and mice exposed to naphthalene by inhalation. The naphthalene part of the model is diffusion limited; the naphthalene oxide part is flow-limited (dashed lines indicate enzymatic reactions by P450 monooxygenase system).

in the naphthalene oxide portion of the current model were the same as those of Quick and Shuler (1999) and Kohn and Melnick (2000).

A sensitivity analysis using Eq. (1) has been performed on the optimized parameters for both rats and mice

$$S_{Yi,Pj}(t_i) = \frac{Y_j(t_i) - Y_0(t_i)}{\delta_j \times Y_0(t_i)}, \quad (1)$$

where $S_P(t)$ is the relative sensitivity for parameter P at time t, $Y_0(t)$ is the nominal value at time t when the model is run with the optimized parameter value, and $Y_j(t)$ is the nominal value at time t when the model is run with an increase or decrease of the optimized parameter value with increment δ.

RESULTS

The optimized parameters used in the naphthalene model are listed in Table 2. The model predicts naphthalene to be rapidly absorbed into the blood during inhalation exposure as a result of the high blood:air partition coefficient and unrestricted permeation. This uptake kinetics was determined by modeling blood time-course data of naphthalene beginning at 12 min after 6 h of inhalation exposure. Metabolic capacity was similar in male and female rats. The metabolic saturation capacity is slightly lower in the female rats. The opposite situation occurs in the model optimizations for the mice in which the K_m in the female mouse is slightly higher than in the male mouse. However, the metabolic capacity in the female mouse model is higher compared to the male mouse. According to the model, the metabolic rate is approximately two- to threefold higher in mice than in rats. The interspecies differences in metabolic capacity are significant and are in accordance with the literature (Buckpitt *et al.*, 1995, 1987).

Even though the current model does not distinguish between the V_{max} and K_m in lung and liver, as the difference in metabolism between the lung and the liver is based on their difference in microsomal protein level, a comparison can still be made between the parameter values presented here and the *in vitro* numbers published in Quick and Shuler (1999). In rats the model shows a higher metabolic capacity compared to the *in vitro* data but a lower saturation capacity. The metabolic capacity in the model is higher compared to the *in vitro* data for the mouse lung and liver. Saturation capacity in the model is the K_m found *in vitro.*

Using the model with a Michaelis–Menten-based metabolic pathway for naphthalene metabolism in both the lung and the liver resulted in a fit to the inhalation data in both species. Alternative models that were used to fit the data (i.e., flow-limited, Hill equations for metabolism, and competitive and noncompetitive inhibition) failed as they, either systematically or alternatively, over- or underpredicted the observed data.

TABLE 1
Physiological Parameters for the PBPK Model of Naphthalene in both Male and Female Rats

	Male rat	Female rat	Male mouse	Female mouse
Body weight (kg)[a]	0.125–0.504	0.1–0.306	0.030	0.024
Cardiac output (L/h/kg$^{0.7}$)	14.7	14.7	11.9	11.9
Ventilation rate (L/h/kg$^{0.7}$)	20	20	24.4	24.4
Tissue volumes (% of body weight)				
Arterial blood[b]	1.8	1.8	2	2
Venous blood[b]	3.6	3.6	4	4
Alveolar space[c]	0.5	0.5	0.5	0.5
Lung[d]	0.52	0.52	0.6	0.6
Liver[e]	3.7	3.7	5.5	5.5
Fat[e]	7.0	7.0	6	6
Kidney[b]	1.48	1.48	1.7	1.7
Other[f]	81.4	81.4	79.7	79.7
Tissue capillary volumes (% of tissue volume)[b,g]				
Lung	18.0	18.0	11	11
Liver	13.8	13.8	11	11
Fat	2.0	2.0	3	3
Kidney	16.0	16.0	10.2	10.2
Other	4.5	4.5	4.2	4.2
Tissue blood flow (% of cardiac output)[b]				
Liver	17.4	17.4	16.2	16.2
Fat	7.0	7.0	5	5
Kidney	14.1	14.1	16.3	16.3
Other[f]	61.5	61.5	62.5	62.5
Partition coefficient[h]				
Blood:air	571	571	571	571
Lung	1.81	1.81	1.81	1.81
Fat	160	160	160	160
Kidney	4	4	4	4
Other	4	4	4	4
Liver	7	7	7	7
Microsomal protein (mg/ml tissue)[i]				
Lung	5.0			
Liver	28			

[a] Changing weights over time, based on weights from 2-year chronic study on naphthalene (NTP, 2000).
[b] Brown *et al.*, 1997.
[c] Davies and Morris (1993).
[d] Schmidt-Nielson (1979).
[e] Average from several literature values.
[f] Calculated residual value.
[g] Altman *et al.* (1970).
[h] Calculated values (Abraham *et al.*, 1985; Fiserova-Bergerova *et al.*, 1984).
[i] Measured values (Quick and Shuler, 1999).

Graphic representations of the fits of the model to male and female rat data are shown in Fig. 2A. The figure shows a good fit to the data with only a slight overprediction of the blood naphthalene concentrations in male rats between 100 and 450 min postexposure for the 30- and 60-ppm doses. Predicted blood naphthalene time courses for the 2-week and 3-, 6-, 12-, and 18-month studies are equivalent (i.e., no apparent sensitivity to the body weight) and therefore data from these exposure durations (which were not significantly different) were combined and presented in single figures for both male and female rats (see Fig. 2B). Here there was a small underprediction of the first four data points in the male rat at the 10-ppm exposure concentration and a small overprediction of the female naphthalene blood concentration at the 60-ppm dose level. The fits of the model to the single-exposure mouse data are shown in Fig. 3. At the 10-ppm dose in male mice the model does not seem to drop fast enough and level off at the same time as the data implicate. However, it should be noted that several measurements of the male (and female) mouse blood naphthalene concentrations were not available due to loss of some animals. As can be seen in Fig. 3, the spread in the data for the female mice tends to be very large (100-fold) at some time points. The iv data were not used to estimate parameter values but were used to validate the model for naphthalene metabolism. Model predictions and the iv data are shown in Fig. 4.

Outcomes of model simulations with regard to tissue concentrations, metabolizing rates, and total metabolism are presented in Table 3. Two time points were chosen at which to report these values; the end of the 6-h exposure period and 24 h after the exposure was started. Modeled steady-state concentrations in the lung at the end of the 6-h exposure period to naphthalene were between 0.2 and 12 μg/ml in the rat (0.5, 3.8, and 12.0 μg/ml in male rat; 0.2, 1.8, and 10.7 μg/ml in female rat at the 10-, 30-, and 60-ppm exposure levels, respectively) and between 0.1 and 1.7 μg/ml in the mouse (0.1 and 1.4 μg/ml in male mouse; 0.3 and 1.7 μg/ml in female mouse at the 10- and 30-ppm exposure levels, respectively) (see Table 3).

As there were no data available on the concentrations of the different naphthalene metabolites in the blood, it was impossible to create a reliable model describing the distribution of these metabolites to the various tissues. Therefore, a previous model for naphthalene oxide metabolism and distribution based on *in vitro* data for epoxide hydrolase and GST activity (Quick and Shuler, 1999) was incorporated into the naphthalene model presented here. According to the model, liver and lung GSH levels drop substantially when exposed to 10, 30, or 60 ppm naphthalene and these changes are similar in male and female rats. The decrease in GSH is larger in the lung than in the liver. The resynthesis of GSH is slower in the lung than in the liver, resulting in incomplete recovery of the GSH concentrations in the lung (see Fig. 5). GSH levels did not return to the initial concentrations after 2 days of no exposure to naphthalene; they remained between 5 and 60% of the initial concentration for the highest and lowest doses, respectively (see Fig. 5, only data for females are shown). In contrast, the model predicts that, in male and female rat liver, the GSH levels do return to their initial levels after a significant decrease during exposure to naphthalene, except for the highest dose exposure,

TABLE 2
Optimized Parameter Values for the PBPK Model of Naphthalene

	Male rat (±SD)	Female rat (±SD)	Male mouse (±SD)	Female mouse (±SD)
Metabolic parameters				
V_{max} (nmol/mg MP/min)	16.5 (0.12)	24.6 (0.5)	38.7 (1.5)	54.8 (2.4)
K_m (nmol/ml)	6.0 (0.13)	3.2 (0.17)	1.5 (0.13)	5.8 (0.40)
Permeability[a]				
Blood:fat	0.14 (3.4e −3)	0.11 (4e −3)	0.20 (10e −3)	0.11 (2e −3)
Blood:other tissues	0.15 (1.5e −3)	0.11 (2e −3)	0.11 (2e −3)	0.19 (10e −3)

[a] Permeability is shown as Perm in the equations.

which returns to about 98% of the initial GSH level (see Fig. 5, only data for females are shown). The male and female mouse also show large decreases in GSH in the lung with exposures to 10- or 30-ppm naphthalene; the decreases in the liver are much less (to only around 70 and 5% of the initial amount for the lowest and highest doses, respectively) (see Fig. 5, only data for females are shown). Similar to the rats, there is a full recovery of GSH levels in the mouse liver within 18 h

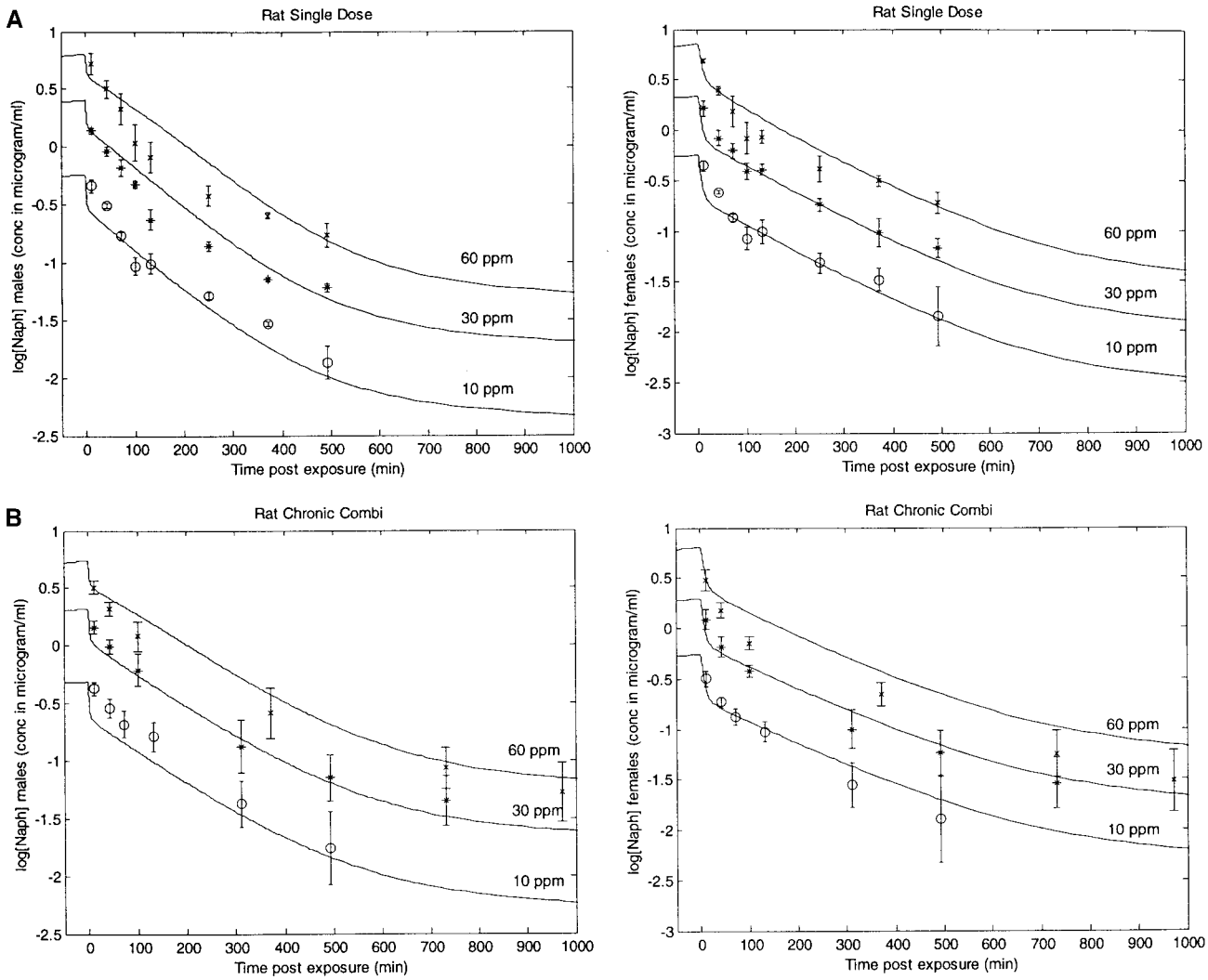

FIG. 2. Blood concentration of naphthalene (mean ± SD, in μg/mL) in male rats (body weight 0.125–0.504 kg) and female rats (body weight 0.1–0.306 kg) immediately after (A) a single 6-h exposure or (B) after exposure for 2 weeks or 3, 6, 12, or 18 months (6 h/day, 5 days/week) to naphthalene by inhalation.

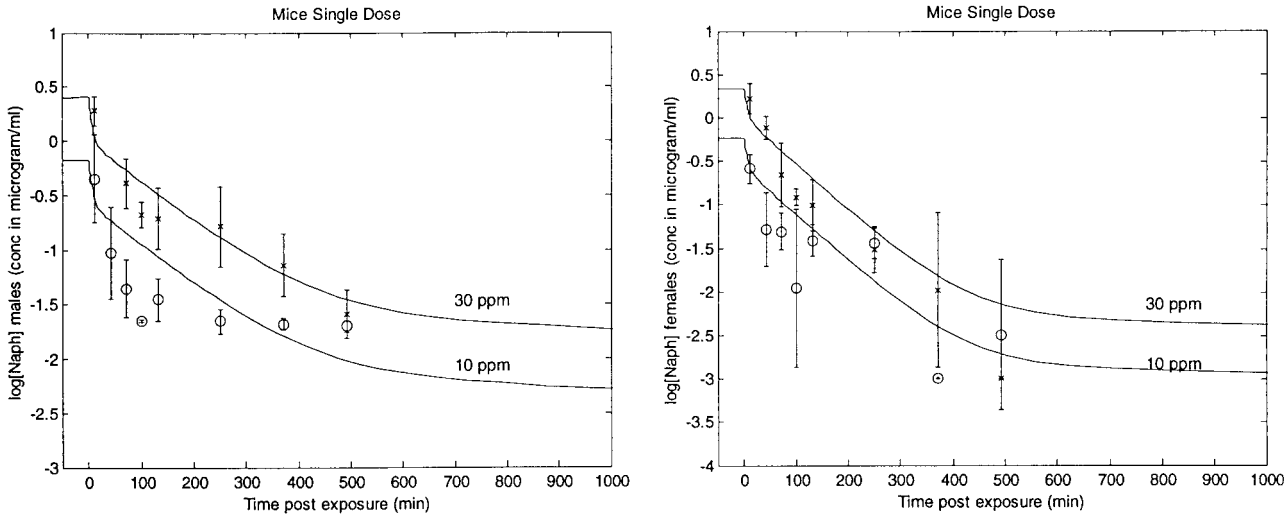

FIG. 3. Blood concentration of naphthalene (mean ± SD, in μg/mL) in male (body weight 0.03 kg) and female (body weight 0.024 kg) mice immediately after a single 7-h exposure to naphthalene by inhalation.

after the 6-h exposure. The recovery in the mouse lung is not complete (65 to 80% of the initial values for the highest and lowest dose, respectively, after 2 days with no exposure to naphthalene).

Predicted naphthalene oxide concentrations in the mouse lung are 1.5-fold higher in the female mouse for the 10- and 30-ppm exposures than in the female rat lung at the same exposure levels (see Fig. 6). This difference is similar when the male mouse lung and the male rat lung are compared (data not shown).

The data in Fig. 7 (only data for females are shown, data for males are similar) show the relative change in the model prediction at the 0.25-, 0.5-, 0.75-, and 1-day time points when the parameter in question is changed by ±10% from its optimized value. As shown in Fig. 7, the model is fairly stable with regard to most of the parameters. The permeability from blood: other tissues and, to a lesser extent, the blood:fat permeability are the parameters of most influence in both rats and mice.

DISCUSSION

A physiologically based toxicokinetic model was developed to characterize the disposition of inhaled and injected naphthalene in rats and mice. This model was used to estimate the amount of naphthalene inhaled by rats and mice (NTP, 1992) at the exposure concentrations used in the 2-year studies of this

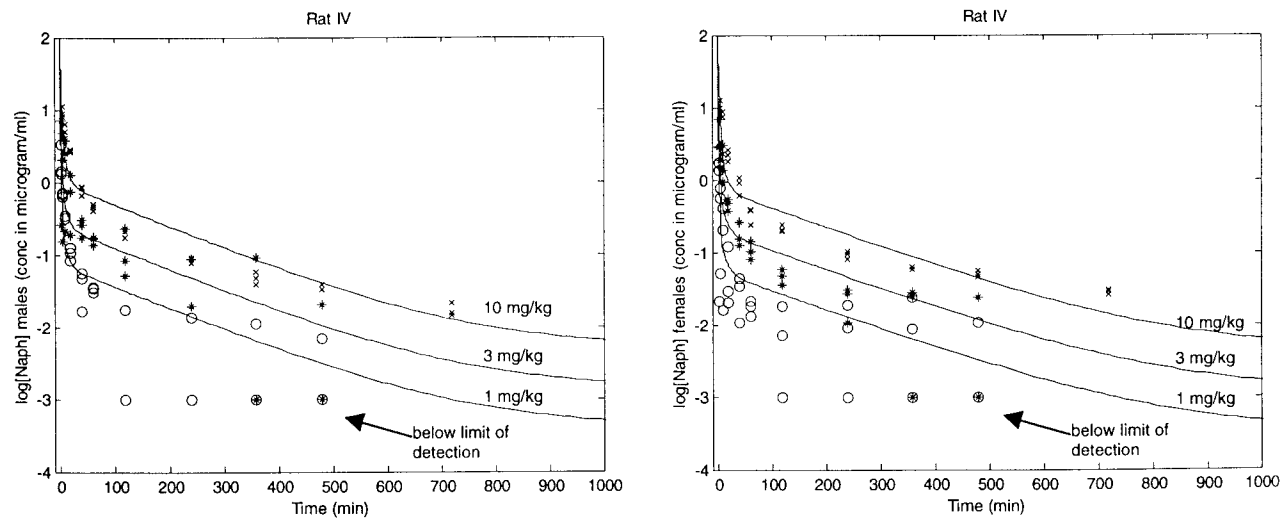

FIG. 4. Blood concentration of naphthalene in male (body weight 0.255 kg) and female (body weight 0.156 kg) rats after an iv dose of naphthalene (the data points in the graph at log[Naph] of −3 are below limit of detection).

TABLE 3
Outcomes of Model Simulations

	Male rat			Female rat			Male mouse		Female mouse	
Amounts of naphthalene	10 ppm	30 ppm	60 ppm	10 ppm	30 ppm	60 ppm	10 ppm	30 ppm	10 ppm	30 ppm
At end of 6 h exposure to naphthalene										
Concentration in lung (μg/ml)	0.5	3.8	12.0	0.2	1.8	10.7	0.1	1.4	0.3	1.7
Metabolic rate lung (mg/h/ml)	0.3	0.5	0.6	0.3	0.8	0.9	0.5	1.3	0.5	1.5
Cumulative metabolism in lung (mg/kg body wt)	6.9	15.1	17.9	8.3	22.1	27.8	15.3	43.2	17.5	48.7
Concentration in liver (μg/ml)	2e −3	1e −2	3e −2	1e −3	2e −3	8e −3	2e −4	7e −4	6e −4	2e −3
Metabolic rate in liver (mg/h/ml)	0.01	0.05	0.1	0.01	0.03	0.1	0.008	0.03	0.01	0.04
Cumulative metabolism in liver (mg/kg body wt)	1.9	7.9	20.4	1.6	5.7	16.9	2.4	7.9	3.1	11.0
At 18 h postexposure (=24 h)										
Cumulative metabolism in lung (mg/kg body wt)	8.5	21.7	33.3	10.0	28.3	45.9	20.9	60.7	22.7	64.9
Cumulative metabolism in liver (mg/kg body wt)	2.3	9.8	26.9	1.9	6.9	21.3	3.2	11.1	3.9	14.4
Total cumulative metabolism (mg/kg body wt)	10.9	31.5	60.2	11.9	35.2	67.2	24.2	71.8	26.6	79.3
Total inhaled (mg/kg body wt)	11.8	35.5	71.1	12.7	38.1	76.3	25.9	77.6	27.6	82.9
Total from blood to alveolar (mg/kg body wt)	0.3	1.1	2.9	0.3	0.9	0.3	0.7	2.5	0.6	2.0
Net inhaled (mg/kg body wt)	11.6	34.5	68.2	12.4	37.2	76.0	25.1	75.1	27.1	80.9
Total metabolism as % of total inhaled	91.9	88.6	84.7	93.6	92.4	88.1	93.5	92.5	96.3	95.6
Total metabolism as % of net inhaled	93.5	91.2	88.3	95.9	94.7	88.4	96.3	95.6	98.3	98.0

Note. Animal body weight: male rat, 125 g; female rat, 100 g; male mouse, 30 g; female mouse, 24 g. Lung tissue volume: male rat, 0.65 ml; female rat, 0.52 ml; male mouse, 0.18 ml; female mouse, 0.14 ml. Liver tissue volume: male rat, 4.64 ml; female rat, 3.72 ml; male mouse, 1.65 ml; female mouse, 1.32 ml.

chemical, the amount of the inhaled dose that was metabolized during the 6-h exposures in rats and mice and during the 18 h following exposure, the steady-state concentrations of naphthalene (reached during exposure) in the liver and lung of rats and mice during chronic exposure, and the rate of naphthalene metabolism in the liver and lung of rats and mice at these steady-state concentrations (see Table 3). In addition, a model that includes metabolism of naphthalene oxide by epoxide hydrolase and glutathione *S*-transferase was utilized to predict lung concentrations of naphthalene oxide in rats and mice exposed to naphthalene and changes in liver and lung concentrations of glutathione.

The model presented in this paper is fairly robust with regard to the optimized parameters (see Fig. 7), and the sensitivity analysis shows that the permeabilities indicating delivery of the parent compound to the tissues are the most important, assuming a low sensitivity to the metabolic parameters V_{max} and K_m.

Approximately 88 to 96% of the absorbed naphthalene is metabolized by rats and 96 to 98% of the inhaled naphthalene is metabolized by mice (see Table 3). These values for the percentage of the inhaled parent compound that is metabolized are greater than those reported for other volatile chemicals (Richardson *et al.*, 1999) and reflect the low vapor pressure of naphthalene and its very high estimated blood-to-air partition coefficient ($P_{blood:air} = 571$). Thus, once naphthalene is absorbed into the general circulation, very little parent compound is eliminated by exhalation. Because essentially all of the naphthalene that is absorbed is metabolized, the values for total cumulative metabolism (presented as mg/kg body weight in Table 3) represent the internalized dose of naphthalene in rats and mice resulting from 6-h exposures. Increased metabolism will tend to increase the gradient in concentration of naphthalene in the alveolar space compared to the lung blood and thus enhance further absorption of the compound. Total naphthalene metabolized (i.e., the internalized dose) was higher for mice exposed to 30 ppm than rats exposed to 60 ppm (see Table 3). This difference is due to the higher ventilation and metabolic rates per kg body weight in mice compared to rats.

The data in Table 3 also show that the steady-state concentration of naphthalene in the lung of rats is not very different from that of mice exposed to equivalent concentrations. Cumulative metabolism of naphthalene in the lung was markedly greater in mice than in rats. Rates of naphthalene metabolism did not increase proportionally with increasing exposure concentration, indicating metabolic saturation in this organ. Metabolic saturation was more evident in the rat lung than in the mouse lung. Naphthalene metabolism was practically the same in the mouse and rat livers. No metabolic saturation was apparent in the liver of rats or mice at the exposed doses. For both species, 65 to 75% of the 24-h metabolic clearance occurred during the 6-h exposure period; only in male and female rat lung in the 60-ppm group was metabolic clearance during exposure reduced to about 50% of the total inhaled dose (see Table 3). This is due to metabolic saturation resulting in greater storage of parent compound in the fat at this exposure concentration.

The single-dose intravenous (iv) injection study (NTP, unpublished data) was used as an independent data source to validate the naphthalene model described in this paper and was therefore not used to optimize the model parameters. The model gave a good fit to the iv data. Quick and Shuler (1999) showed a good fit to these same data, especially at the 10

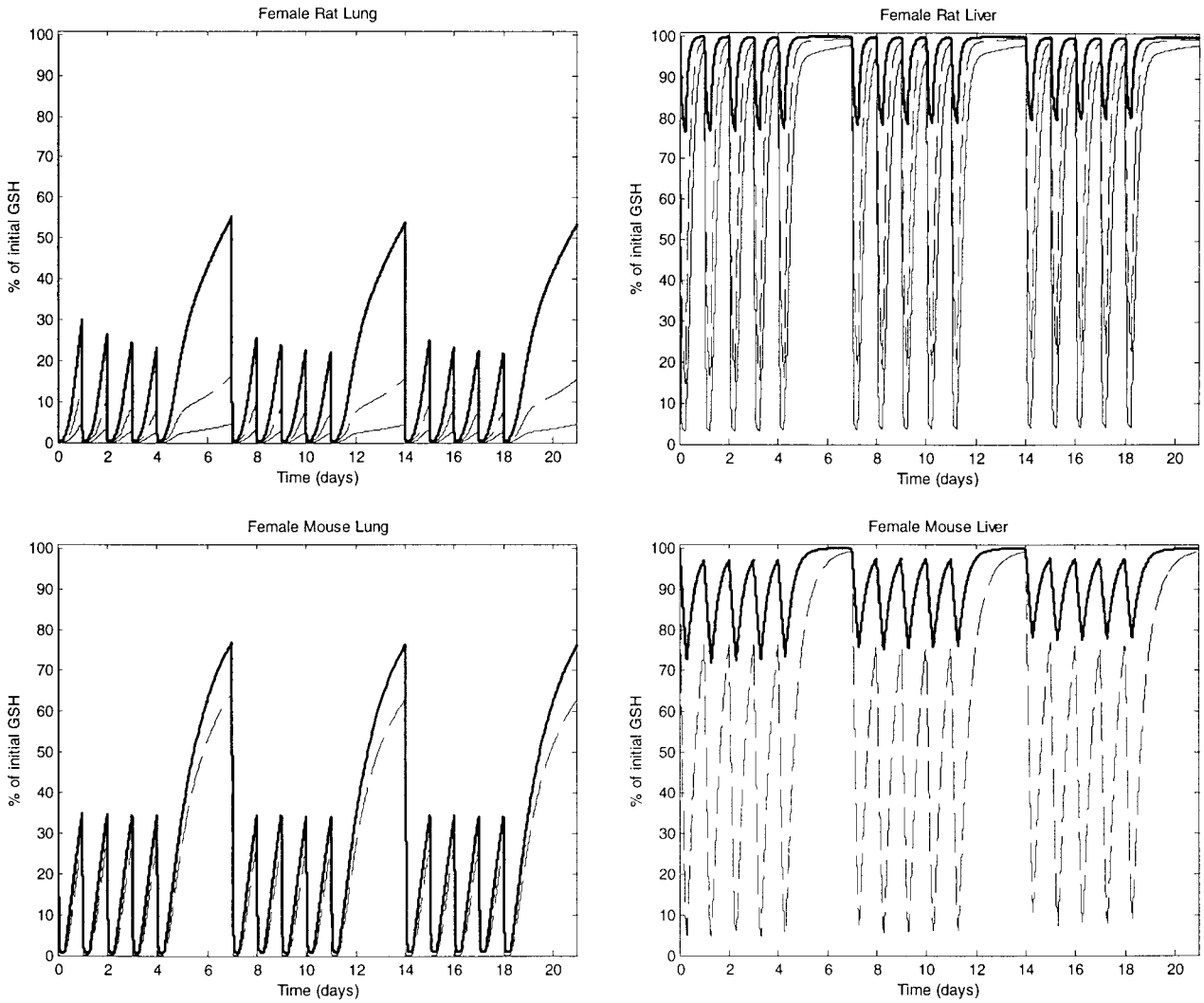

FIG. 5. Model predictions for glutathione levels in the female rat (assumed body weight 0.1–0.17 kg) and female mouse (assumed body weight 0.024 kg) tissues as a percentage of the initial concentration (male levels are not shown but are similar to the female levels) (—— 10 ppm, - - - 30 ppm, —— 60 ppm).

mg/kg dose level at which the current model seems to not have fast enough metabolism in the middle range time points. However, when the predictions of Quick and Shuler's model and parameter values were compared to the inhalation data (which is also the most predominant route of exposure to humans) from the NTP (2000) study, the naphthalene concentrations in the blood were overpredicted at all time points.

The results from the toxicokinetic model of naphthalene indicate that tissue dosimetry of parent compound alone does not explain why this chemical is carcinogenic to the female mouse lung but not to the rat lung. For example, female rats exposed to 60 ppm naphthalene had a higher steady-state concentration of naphthalene in the lung than did female mice exposed to 30 ppm, yet only mice developed lung tumors (NTP, 2000). Although the rates of naphthalene metabolism in the mouse lung are higher than those in the rat lung, according to the model, the detoxification of naphthalene oxide is faster in mice than in rats. The net effect of activation and detoxification was that higher levels of naphthalene oxide were estimated by the model in the lung of mice exposed to 30 ppm naphthalene vs the lung of rats exposed to 60 ppm naphthalene (see Fig. 6). This dosimetry difference may contribute in part to the species difference in lung tumor response to naphthalene exposure, along with a higher sensitivity of the mouse lung to metabolically activated lung toxicants (Shultz *et al.*, 2001). There is also the suggestion that naphthoquinone, formed by P450 from naphthol, instead of naphthalene epoxide can act as a toxicant by covalently binding to proteins (Ghanem and Shuler, 2000; Wilson *et al.*, 1996).

Naphthalene oxide is the primary metabolite formed by cytochrome P450-mediated oxidation of naphthalene. Mice appear to be more susceptible to lung neoplasm induction by epoxide and epoxide-forming chemicals than are rats (Melnick and Huff, 1993). Most notable in this respect is the finding that

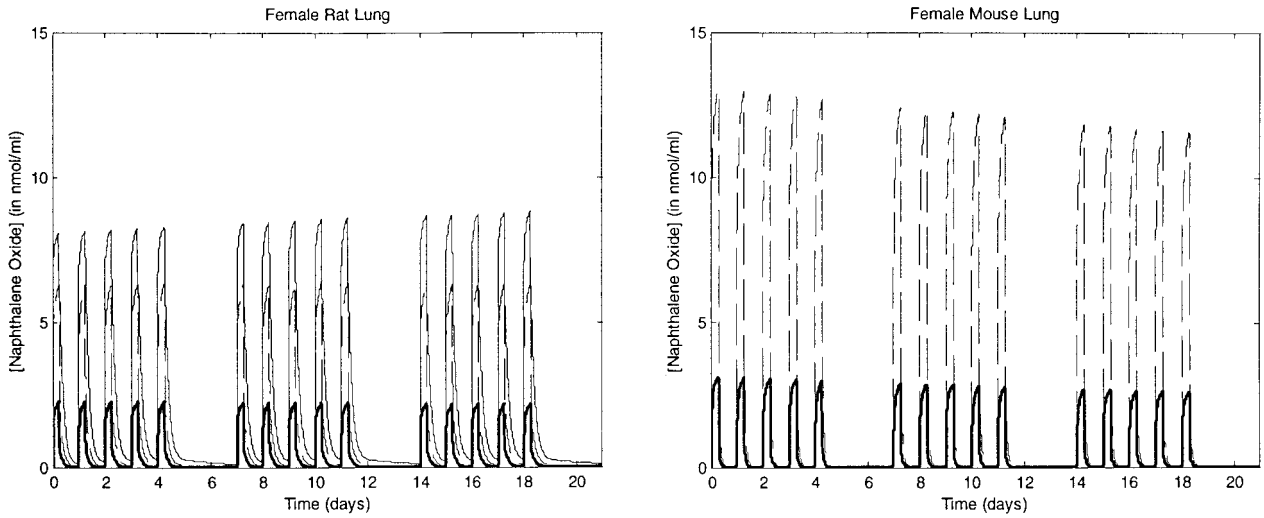

FIG. 6. Model predictions for naphthalene oxide concentrations (in nmol/ml) in the female rat (assumed body weight 0.1–0.17 kg) and female mouse lung (assumed body weight 0.024 kg) (male levels are not shown but are similar to the female levels) (—— 10 ppm, - - - 30 ppm, —— 60 ppm).

inhalation exposure to ethylene oxide induced lung neoplasms in mice (NTP, 1987) but not in rats (Lynch *et al.*, 1984; Snellings *et al.*, 1984). The NTP (1992) study found tumors in the female mouse lung after inhalation exposure to naphthalene. Seven percent of the animals in the control group, 3% of the animals in the 10-ppm dose group, and 21% of the animals in the 30-ppm dose group developed lung tumors. There was no increase in lung tumors found in the rat after inhalation exposure to 10, 30, or 60 ppm naphthalene (NTP, 2000). Thus, if naphthalene oxide is the intermediate responsible for lung neoplasm induction in mice exposed to naphthalene, then the species difference in response at this site may be due to a combination of higher levels of naphthalene oxide in the mouse lung and a greater susceptibility of the mouse lung to epoxide-induced carcinogenesis.

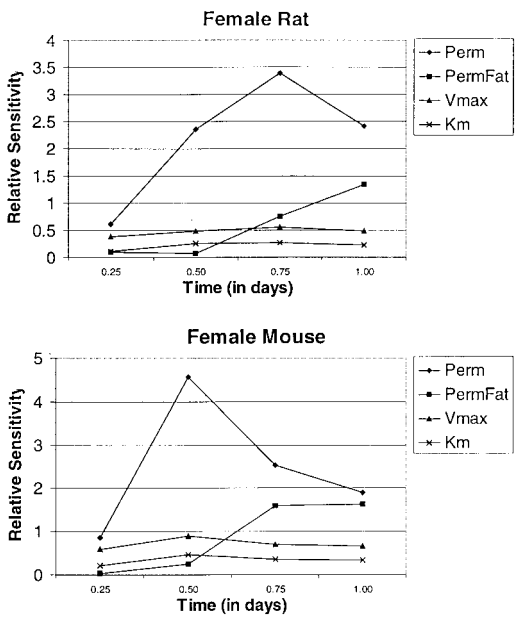

FIG. 7. The relative sensitivity over time of modeled blood naphthalene concentrations with respect to variations in the optimized parameters in female rat and mouse models (male numbers are not shown but are similar to the female numbers). Perm is permeability blood:other tissues; PermFat is permeability blood:fat.

There is evidence that cytochrome P450 and epoxide hydrolase can form a transient complex whereby the formed epoxide is transferred directly to epoxide hydrolase in competition with release into the cytoplasm. This phenomenon has been described for naphthalene (Oesch and Daly, 1972) and modeled for 1,3-butadiene (Kohn and Melnick, 2000). If sufficient data (blood time-course data for naphthalene oxide) were available to introduce the functionality of such a privileged access model into the current naphthalene model, the predictions for naphthalene oxide tissue levels in the rat and mouse lung would likely decrease substantially. A certain amount of the epoxide would be metabolized immediately instead of first being released into the cytoplasm and subsequently metabolized by epoxide hydrolase. Modeling the effectiveness of this privileged access model in rats and mice could contribute to a better understanding of species differences in response to naphthalene exposure.

Another aspect of exposure to naphthalene is the occurrence of nasal toxicity in rats and mice of both sexes. Rats develop nasal tumors, but mice do not. However there are no data available from this study or in the literature on nasal deposition and epithelial absorption of naphthalene. This makes it impossible to create a reliable model for nasal cavity absorption and tissue dosimetry at this time.

More information on time-dependent blood and tissue concentrations of naphthalene metabolites and tissue GSH concentrations would be helpful in identifying the source of the

difference in toxicity of naphthalene in mice and rats. However, conclusions regarding which metabolites may be responsible for naphthalene toxicity could not be reached solely based on the available blood time-course data. Finally, direct measurements of partition coefficient constants might greatly enhance the validity of the naphthalene model.

APPENDIX 1: NOTATION

Concentration

Dose	chamber concentration of naphthalene (nmol/ml) (dose has been converted from ppm to nmol/ml)
AMT_{air}	amount in the air (nmol)
AMT_{alv}	amount in the alveolar space (nmol)
AMT_{art}	amount in the arterial blood (nmol)
AMT_{ven}	amount in the venous blood (nmol)
$AMT_{tissuecap}$	amount in the tissue capillary blood (nmol)
AMT_{tissue}	amount in the tissue (nmol)
V	volume of tissue or blood (ml)

Flow

Q_{vent}	ventilation rate (ml/min)
Q_{total}	total blood flow (ml/min)
Q_{tissue}	blood flow to the tissue (ml/min)

Partition Coefficient and Permeability Constant

$Perm_i$	capillary permeability constant (unitless) =extraction ratio/(1 − extraction ratio) (i = fat, other tissues)
P_{tissue}	tissue:blood partition coefficient
P_{air}	blood:air partition coefficient

Metabolism Rates

V_{max}	maximum velocity of saturable metabolism (nmol/mg MP/min)
K_m	Michaelis–Menten constant for metabolism (nmol/ml)
MP_j	amount of microsomal protein (mg/ml tissue) (j = lung, liver)

APPENDIX 2: PBPK DIFFERENTIAL EQUATIONS

Chamber

$$\frac{dAMT_{air}}{dt} = -Dose \times Q_{vent} + \frac{AMT_{alv}}{V_{alv}} \times Q_{vent}$$

Alveolar Space

$$\frac{dAMT_{alv}}{dt} = Dose \times Q_{vent} + \frac{AMT_{lungcap}}{V_{lungcap}} \times \frac{Q_{vent}}{P_{air}} - \frac{AMT_{alv}}{V_{alv}} \times Q_{vent} - \frac{AMT_{alv}}{V_{alv}} \times Q_{vent}$$

Arterial Blood

$$\frac{dAMT_{art}}{dt} = \frac{AMT_{lungcap}}{V_{lungcap}} \times Q_{total} - \frac{AMT_{art}}{V_{art}} \times Q_{total}$$

Lung

$$\frac{dAMT_{lungcap}}{dt} = \frac{AMT_{ven}}{V_{ven}} \times Q_{total} + \frac{AMT_{alv}}{V_{alv}} \times Q_{vent} + \frac{AMT_{lung}}{V_{lung}} \times \frac{Q_{total}}{P_{lung}} \times Perm_i - \frac{AMT_{lungcap}}{V_{lungcap}} \times Q_{total} - \frac{AMT_{lungcap}}{V_{lungcap}} \times Q_{total} \times Perm_i - \frac{AMT_{lungcap}}{V_{lungcap}} \times \frac{Q_{vent}}{P_{air}}$$

$$\frac{dAMT_{lung}}{dt} = \frac{AMT_{lungcap}}{V_{lungcap}} \times Q_{total} \times Perm_i - \frac{AMT_{lung}}{V_{lung}} \times \frac{Q_{total}}{P_{lung}} \times Perm_i - \frac{V_{max} \times V_{lung} \times AMT_{lung}}{K_m \times V_{lung} + AMT_{lung}} \times MP_j$$

Venous Blood

$$\frac{dAMT_{ven}}{dt} = \sum \frac{AMT_{tissuecap}}{V_{tissuecap}} \times Q_{tissue} - \frac{AMT_{ven}}{V_{ven}} \times Q_{total}$$

Liver

$$\frac{dAMT_{livercap}}{dt} = \frac{AMT_{art}}{V_{art}} \times Q_{liver} + \frac{AMT_{liver}}{V_{liver}} \times \frac{Q_{liver}}{P_{liver}} \times Perm_i - \frac{AMT_{livercap}}{V_{livercap}} \times Q_{liver} - \frac{AMT_{livercap}}{V_{livercap}} \times Q_{liver} \times Perm_i$$

$$\frac{dAMT_{liver}}{dt} = \frac{AMT_{livercap}}{V_{livercap}} \times Q_{liver} \times Perm_i - \frac{AMT_{liver}}{V_{liver}} \times \frac{Q_{liver}}{P_{liver}} \times Perm_i - \frac{V_{max} \times V_{liver} \times AMT_{liver}}{K_m \times V_{liver} + AMT_{liver}} \times MP_j$$

Fat, Kidney, and Other (Nonmetabolizing Tissues)

$$\frac{dAMT_{tissuecap}}{dt} = \frac{AMT_{art}}{V_{art}} \times Q_{tissue} + \frac{AMT_{tissue}}{V_{tissue}} \times \frac{Q_{tissue}}{P_{tissue}} \times Perm_i - \frac{AMT_{tissuecap}}{V_{tissuecap}} \times Q_{tissue} - \frac{AMT_{tissuecap}}{V_{tissuecap}} \times Q_{tissue} \times Perm_i$$

$$\frac{dAMT_{tissue}}{dt} = \frac{AMT_{tissuecap}}{V_{tissuecap}} \times Q_{tissue} \times Perm_i - \frac{AMT_{tissue}}{V_{tissue}} \times \frac{Q_{tissue}}{P_{tissue}} \times Perm_i$$

REFERENCES

Abraham, M. H., Kamlet, M. J., Taft, R. W., Doherty, R. M., and Weathersby, P. K. (1985). Solubility properties in polymers and biological media. 2. The

correlation and prediction of the solubilities of nonelectrolytes in biological tissues and fluids. *J. Med. Chem.* **28,** 865–870.

Altman, P. L., Katz, D. D., and Federation of American Societies for Experimental Biology. Committee on Biological Handbooks (1970). *Respiration and Circulation.* Federation of American Societies for Experimental Biology Committee on Biological Handbooks, Bethesda, MD.

ATSDR (1990). *Toxicological Profile for Naphthalene and 2-Methylnaphthalene.* U.S. Agency for Toxic Substances and Disease, Atlanta, GA.

Bjorseth, A., Bjorseth, O., and Fjeldstad, P. E. (1978). Polycyclic aromatic hydrocarbons in the work atmosphere. I. Determination in an aluminum reduction plant. *Scand. J. Work Environ. Health* **4,** 212–223.

Brown, R. P., Delp, M. D., Lindstedt, S. L., Rhomberg, L. R., and Beliles, R. P. (1997). Physiological parameter values for physiologically based pharmacokinetic models. *Toxicol. Ind. Health* **13,** 407–484.

Buckpitt, A., Chang, A. M., Weir, A., Van Winkle, L., Duan, X., Philpot, R., and Plopper, C. (1995). Relationship of cytochrome P450 activity to Clara cell cytotoxicity. IV. Metabolism of naphthalene and naphthalene oxide in microdissected airways from mice, rats, and hamsters. *Mol. Pharmacol.* **47,** 74–81.

Buckpitt, A. R., Castagnoli, N., Jr., Nelson, S. D., Jones, A. D., and Bahnson, L. S. (1987). Stereoselectivity of naphthalene epoxidation by mouse, rat, and hamster pulmonary, hepatic, and renal microsomal enzymes. *Drug Metab. Dispos.* **15,** 491–498.

CEDRA (1994). *Biological Sample Method Development Report for Naphthalene in Rodent Blood.* CEDRA DCN, Austin, TX.

Davies, B., and Morris, T. (1993). Physiological parameters in laboratory animals and humans [editorial]. *Pharm. Res.* **10,** 1093–1095.

D'Souza, R. W., and Boxenbaum, H. (1988). Physiological pharmacokinetic models: Some aspects of theory, practice and potential. *Toxicol. Ind. Health* **4,** 151–171.

Fiserova-Bergerova, V., Tichy, M., and Di Carlo, F. J. (1984). Effects of biosolubility on pulmonary uptake and disposition of gases and vapors of lipophilic chemicals. *Drug Metab. Rev.* **15,** 1033–1070.

Ghanem, A., and Shuler, M. L. (2000). Combining cell culture analogue reactor designs and PBPK models to probe mechanisms of naphthalene toxicity. *Biotechnol. Prog.* **16,** 334–345.

Hansch, C., Hoekman, D., Leo, A., Zhang, L., and Li, P. (1995). The expanding role of quantitative structure–activity relationships (QSAR) in toxicology. *Toxicol. Lett.* **79,** 45–53.

Hoang, K. (1995). Physiologically based pharmacokinetic models: Mathematical fundamentals and simulation implementations. *Toxicol. Lett.* **79,** 99–106.

Kanekal, S., Plopper, C., Morin, D., and Buckpitt, A. (1991). Metabolism and cytotoxicity of naphthalene oxide in the isolated perfused mouse lung. *J. Pharmacol. Exp. Ther.* **256,** 391–401.

Kohn, M. C. (1997). The importance of anatomical realism for validation of physiological models of disposition of inhaled toxicants. *Toxicol. Appl. Pharmacol.* **147,** 448–458.

Kohn, M. C., and Melnick, R. L. (2000). The privileged access model of 1,3-butadiene disposition. *Environ. Health Perspect.* **108**(Suppl. 5), 911–917.

Kotz, S., and Johnson, N. L. (1983). *Encyclopedia of Statistical Sciences.* Wiley, New York.

Lyman, W. J., Reehl, W. F., and Rosenblatt, D. H. (1990). *Handbook of Chemical Property Estimation Methods.* American Chemical Society, Washington, DC.

Lynch, D. W., Lewis, T. R., Moorman, W. J., Burg, J. R., Groth, D. H., Khan, A., Ackerman, L. J., and Cockrell, B. Y. (1984). Carcinogenic and toxicologic effects of inhaled ethylene oxide and propylene oxide in F344 rats. *Toxicol. Appl. Pharmacol.* **76,** 69–84.

Mahvi, D., Bank, H., and Harley, R. (1977). Morphology of a naphthalene-induced bronchiolar lesion. *Am. J. Pathol.* **86,** 558–572.

Melnick, R. L., and Huff, J. E. (1993). 1,3-Butadiene induces cancer in experimental animals at all concentrations from 6.25 to 8000 parts per million. *IARC Sci. Publ.* **127,** 309–322.

NTP (1987). *Toxicology and Carcinogenesis Studies of Ethylene Oxide (CAS No. 75-21-8) in B6C3F1 Mice (Inhalation Studies).* U.S. Dept. Health and Human Services, Public Health Service, National Institutes of Health, Research Triangle Park, NC.

NTP (1992). *Toxicology and Carcinogenesis Studies of Naphthalene (CAS No. 91-20-3) in B6C3F1 Mice (Inhalation Studies).* U.S. Dept. Health and Human Services, Public Health Service, National Institutes of Health, Research Triangle Park, NC.

NTP (2000). *Draft NTP Technical Report on the Toxicology and Carcinogenesis Studies of Naphthalene (CAS No. 91-20-3) in F344/N Rats (Inhalation Studies).* U.S. Dept. Health and Human Services, Public Health Service, National Institutes of Health, Research Triangle Park, NC.

Oesch, F., and Daly, J. (1972). Conversion of naphthalene to *trans*-naphthalene dihydrodiol: Evidence for the presence of a coupled aryl monooxygenase-epoxide hydrase system in hepatic microsomes. *Biochem. Biophys. Res. Commun.* **46,** 1713–1720.

Plopper, C. G., Suverkropp, C., Morin, D., Nishio, S., and Buckpitt, A. (1992). Relationship of cytochrome P-450 activity to Clara cell cytotoxicity. I. Histopathologic comparison of the respiratory tract of mice, rats and hamsters after parenteral administration of naphthalene. *J. Pharmacol. Exp. Ther.* **261,** 353–363.

Quick, D. J., and Shuler, M. L. (1999). Use of in vitro data for construction of a physiologically based pharmacokinetic model for naphthalene in rats and mice to probe species differences. *Biotechnol. Prog.* **15,** 540–555.

Richardson, K. A., Peters, M. M., Wong, B. A., Megens, R. H., van Elburg, P. A., Booth, E. D., Boogaard, P. J., Bond, J. A., Medinsky, M. A., Watson, W. P., and van Sittert, N. J. (1999). Quantitative and qualitative differences in the metabolism of ^{14}C-1,3-butadiene in rats and mice: Relevance to cancer susceptibility. *Toxicol. Sci.* **49,** 186–201.

Schmeltz, I., Tosk, J., and Hoffmann, D. (1976). Formation and determination of naphthalenes in cigarette smoke. *Anal. Chem.* **48,** 645–650.

Schmidt-Nielson, K. (1979). *Animal Physiology: Adaptation and Environment.* Cambridge Univ. Press, New York.

Shultz, M. A., Morin, D., Chang, A. M., and Buckpitt, A. (2001). Metabolic capabilities of CYP2F2 with various pulmonary toxicants and its relative abundance in mouse lung subcompartments. *J. Pharmacol. Exp. Ther.* **296,** 510–519.

Sittig, M. (1980). Naphthalene. In *Priority Pollutants* (M. Sittig, ed.), pp. 273–276. Noyes Data Corporation, Park Ridge, NJ.

Snellings, W. M., Weil, C. S., and Maronpot, R. R. (1984). A two-year inhalation study of the carcinogenic potential of ethylene oxide in Fischer 344 rats. *Toxicol. Appl. Pharmacol.* **75,** 105–117.

Sweeney, L. M., Shuler, M. L., Quick, D. J., and Babish, J. G. (1996). A preliminary physiologically based pharmacokinetic model for naphthalene and naphthalene oxide in mice and rats. *Ann. Biomed. Eng.* **24,** 305–320.

The Mathworks (1999). MATLAB. The Mathworks, Natick, MA.

Tong, S. S., Hirokata, Y., Trush, M. A., Mimnaugh, E. G., Ginsburg, E., Lowe, M. C., and Gram, T. E. (1981). Clara cell damage and inhibition of pulmonary mixed-function oxidase activity by naphthalene. *Biochem. Biophys. Res. Commun.* **100,** 944–950.

Wilson, A. S., Davis, C. D., Williams, D. P., Buckpitt, A. R., Pirmohamed, M., and Park, B. K. (1996). Characterisation of the toxic metabolite(s) of naphthalene. *Toxicology* **114,** 233–242.